NRC Research Press

ARTICLE

Investigating spatial variation and temperature effects on maturity of female winter flounder (*Pseudopleuronectes americanus*) using generalized additive models

Megan V. Winton, Mark J. Wuenschel, and Richard S. McBride

Abstract: Generalized additive models were used to investigate fine-scale spatial variation in female maturity across the three United States' winter flounder (*Pseudopleuronectes americanus*) stocks. The effect of temperature on maturity was also investigated. Maturity models explicitly incorporating spatial structure performed better than "traditional" methods incorporating spatial effects by aggregating data according to predefined stock boundaries. Models including temperature explained more of the variability in maturity than those based only on fish size or age but did not improve fit over models incorporating spatial structure. Based on the size- and age-at-maturity estimates from the spatially explicit models, distinct subareas were objectively identified using a spatially constrained clustering algorithm. The results suggested greater variation in size- and age-at-maturity within than between existing stock areas. The approach outlined here provides a method for identifying areas with different vital rates without the need to presume subjective boundaries.

Résumé : Des modèles additifs généralisés ont été utilisés pour examiner les variations spatiales fines de la maturité des femelles dans les trois stocks de plie rouge (*Pseudopleuronectes americanus*) des États-Unis. L'effet de la température sur la maturité a également été examiné. Les modèles de maturité qui intègrent explicitement la structure spatiale donnent de meilleurs résultats que les méthodes « traditionnelles » qui intègrent les effets spatiaux en groupant les données selon des limites de stock prédéfinies. Les modèles intégrant la température expliquent une plus grande part de la variabilité de la maturité que ceux qui ne reposent que sur la taille ou l'âge des poissons, bien qu'ils n'améliorent pas le calage sur les observations par rapport aux modèles intégrant la structure spatiale. À la lumière des estimations de la taille et de l'âge à la maturité obtenues des modèles spatialement explicites, différentes sous-régions ont été délimitées objectivement à l'aide d'un algorithme de groupement intégrant des contraintes spatiales. Les résultats semblent indiquer de plus grandes variations de la taille et de l'âge à la maturité à l'intérieur des régions des stocks existants qu'entre ces différentes régions. L'approche décrite constitue une méthode permettant de cerner des régions présentant différents taux vitaux sans nécessiter la définition préalable de limites subjectives. [Traduit par la Rédaction]

Introduction

Winter flounder (*Pseudopleuronectes americanus*) is a commercially valuable member of the groundfish assemblage of the Northwest Atlantic Ocean. The species has been recorded in shelf waters from North Carolina, USA, to Labrador, Canada, over almost 20° latitude (Pereira et al. 1999); however, its exploitable range is largely limited to areas north of New Jersey (DeCelles and Cadrin 2011). Within United States' (US) waters, winter flounder are managed as three stocks: the Gulf of Maine (GOM), southern New England and Mid-Atlantic (SNE), and Georges Bank (GB). This rationale is based on differences in meristics, life history characteristics, and movement patterns (DeCelles and Cadrin 2011; Northeast Fisheries Science Center 2011). Recent studies have reported evidence of substantial variation in maturity schedules within stock regions (McBride et al. 2013), which suggests the need to assess such variation at a finer spatial scale.

Reported variation in life history parameters and spawning times among the three US winter flounder stocks suggests that temperature is likely one of the key factors driving observed differences. With the exception of the offshore GB stock, which exhibits faster growth and larger sizes-at-maturity than the two inshore stocks (Pereira et al. 1999; McBride et al. 2013), trends in winter flounder life history parameters generally follow a latitudinal pattern paralleling along-shore temperature gradients. Fish at the southern end of the species' exploitable US range tend to grow faster and mature at earlier ages (estimated median age at maturity of 2.4 years) than those in the northern GOM (4.7 years; McBride et al. 2013). The timing of spawning follows a similar gradient, with fish in SNE and GB stock areas spawning earlier in the species' winter-to-spring spawning season (November–April) than those in the GOM (April–June; Pereira et al. 1999; Press et al. 2014). These latitudinal trends continue into Canadian waters, where the median estimated age-at-maturity increases to 7.0 years for female flounder off of Newfoundland (Kennedy and Steele 1971).

The role of temperature in regulating enzymatic activity, and hence metabolism and growth, is well documented in ectotherms (Kingsolver 2009). Linear functions based on temperature have been successfully applied to explain intraspecies variation in

Received 27 November 2013. Accepted 20 April 2014.

Paper handled by Associate Editor Yong Chen.

M.V. Winton.* Integrated Statistics, 172 Shearwater Way, Falmouth, MA 02540, USA.
M.J. Wuenschel and R.S. McBride. Northeast Fisheries Science Center, National Marine Fisheries Service, Woods Hole Laboratory, 166 Water Street, Woods Hole, MA 02543, USA.
Corresponding author: Megan V. Winton (e-mail: megan.winton@gmail.com).
*Present address: Coonamessett Farm Foundation, 277 Hatchville Road, East Falmouth, MA 02536, USA.

growth in both laboratory and wild fish populations at temperatures within a species' preferred range (Brander 1995; Neuheimer and Taggart 2007). However, the efficacy of such metrics breaks down near the extremes of a species' tolerated temperature range, where the relationship becomes nonlinear (Kingsolver 2009). Inshore stocks of winter flounder inhabit coastal waters and estuaries (Pereira et al. 1999), where they may encounter both low (particularly in GOM) and high (particularly in SNE) temperature stress; therefore nonlinear functions are likely required to adequately describe temperature effects on growth and maturity.

Generalized linear models (GLMs) are typically used to estimate size- and age-at-maturity in fish stocks. While spatial structure can be incorporated into GLMs via inclusion of geographic coordinates, model specification and prediction over continuous areas can be quite complicated, or even impossible, depending on the spatial distribution of data (Wood 2006). For this reason, inter- and intrastock variation is often assessed by treating region as a categorical variable rather than explicitly incorporating spatial coordinates (e.g., McBride et al. 2013). Generalized additive models (GAMs) are nonparametric analogues to GLMs that allow for the incorporation of nonlinear terms through the application of smoothing functions, facilitating spatially explicit extensions of the models typically used to estimate maturity. Importantly, this approach does not require the imposition of subjective boundaries to estimate parameters on regional scales, which may mask fine-scale, local variation.

Owing to their inherent flexibility, GAMs are also better suited to modeling nonlinear responses to environmental variables such as temperature. Such models have been applied to relate indices of abundance and catch data to environmental conditions over large geographic areas for several fish stocks (Manderson et al. 2011; Smart et al. 2012; Augustin et al. 2013), but have yet to be applied to life history parameters in the same context. The objectives of this study were to (*i*) investigate variation in maturity of female winter flounder in US waters using spatially explicit GAMs and compare the results with those obtained using "traditional" models, (*ii*) evaluate potential temperature effects, and (*iii*) identify distinct regions characterized by similar maturity schedules via the application of spatially constrained cluster analysis methods.

Materials and methods

Sample collection

Female winter flounder were collected from all three US stock areas during marine resource surveys conducted by the Northeast Fisheries Science Center (NEFSC), the New Jersey Department of Environmental Protection (NJDEP), the Massachusetts Division of Marine Fisheries (MADMF), the Maine Department of Marine Resources (MEDMR), and the Connecticut Department of Environmental Protection (CTDEP) from March 2007 to June 2012 ($n = 1614$; Fig. 1). All surveys followed a stratified, random design and employed bottom otter trawls with lined cod ends to retain smaller fish (Byrne 1994; Reid et al. 1999; Chen et al. 2006; NEFSC Vessel Calibration Working Group 2007; King et al. 2010). All samples were collected immediately preceding or during the spawning season (winter to spring), when maturity is unambiguous, to mitigate potential differences in the estimated size- and age-at-maturity due to time of year. Data collected from 2007 to 2010 ($n = 633$) were previously reported in McBride et al. (2013).

Fish were sampled at sea immediately following each otter trawl tow. For tows with large numbers of winter flounder, subsampling was based on a length-stratified design. On several occasions, fish collected during MADMF surveys were collected whole, stored on ice, and processed at the NEFSC the day after collection. With the exception of fish collected during NEFSC surveys, total length (TL) was measured to the nearest millimetre; flounder collected on NEFSC surveys during 2007–2011 were measured to the nearest centimetre and those during 2012 to the nearest 0.5 cm. Total mass and gonad mass of each fish were determined to the nearest 1 g. An approximately 1 cm^3 sample was excised from the middle of one ovarian lobe and preserved in 10% buffered formalin for a period of at least 1 month.

Otoliths were collected for age estimation following the methods of Penttila and Dery (1988), using 1 January as the universal birth date. Age was estimated for 1443 of the flounder sampled. The NEFSC aged the majority of fish from all five surveys ($n = 1076$). A subsample collected in the GOM was aged by MEDMR staff as part of their ongoing monitoring program ($n = 367$). Preliminary analyses indicated that the probability of maturity-at-age did not differ between ageing agencies (see online supplementary material for details; Table S1; Fig. S1[1]); therefore, ages from both the NEFSC and MEDMR were used in the final analysis.

Maturity determination

Given the potential for maturity misclassification using macroscopic methods (McBride et al. 2013), final maturity classification was assigned based on gonad histology criteria. Fixed ovarian tissue was prepared following a standard paraffin embedding protocol and stained using Schiffs–Mallory trichrome or hematoxylin–eosin (Press et al. 2014). Prepared sections were viewed using a compound microscope (40×–100×) and staged following McBride et al. (2013). Given that fish were sampled in close proximity to the peak spawning period, first-time maturing fish would not spawn until the following year because of the (approximate) 1-year time course of oocyte development (Press et al. 2014). Therefore, we reduced the 10 maturity classes of McBride et al. (2013) to two functional classes: immature (stages 1 and 2; Table 1) and mature (stages 3–10).

Maturity models

What we herein refer to as "traditional" maturity models estimate the probability of a fish being mature as a function of size or age using a GLM fitted to binomial maturity data (0 = immature; 1 = mature). A binomial error distribution and a logit link function, which defines the relationship between the response variable and the linear predictor, are conventionally assumed. The expected proportion of fish mature at size or age i, $E(y_i) = \mu_i$, is estimated as

$$(1) \qquad \text{logit}(\mu_i) = \beta_0 + \beta_1 x_i$$

where β_0 is an intercept term, β_1 is a regression parameter, and x_i is size or age. While geographic coordinates can be directly incorporated into such models, the complexity of location effects is often not well represented by linear functions; therefore, potential differences between stock or other areas of interest are more typically considered by incorporating geographic area as a categorical variable:

$$(2) \qquad \text{logit}(\mu_{ij}) = \beta_0 + \beta_1 x_i \times \text{Area}_j$$

where "×" indicates an interaction term and each fish is assigned to an area j (which may be a stock area or some other predefined boundary) based on the collection location.

GAMs are nonparametric analogues to GLMs that allow for the incorporation of nonlinear effects of covariates on the response variable, facilitating spatially explicit extensions of the maturity models described above. Interaction terms between nonlinear

[1]Supplementary data are available with the article through the journal Web site at http://nrcresearchpress.com/doi/suppl/10.1139/cjfas-2013-0617.

Fig. 1. Collection locations of female winter flounder sampled from 2007 to 2012. Samples are grouped by collecting agency: Maine Department of Marine Resources (MEDMR, n = 587); Massachusetts Division of Marine Fisheries (MADMF, n = 431); Northeast Fisheries Science Center (NEFSC, n = 370); Connecticut Department of Environmental Protection (CTDEP, n = 69); and New Jersey Department of Environmental Protection (NJDEP, n = 157). Boundaries for the three US stock areas are indicated by black lines. Grey contour lines trace the 50 and 100 m isobaths. US state names are coded as follows: CT = Connecticut; MA = Massachusetts; ME = Maine; NH = New Hampshire; NJ = New Jersey; NY = New York; RI = Rhode Island; VT = Vermont.

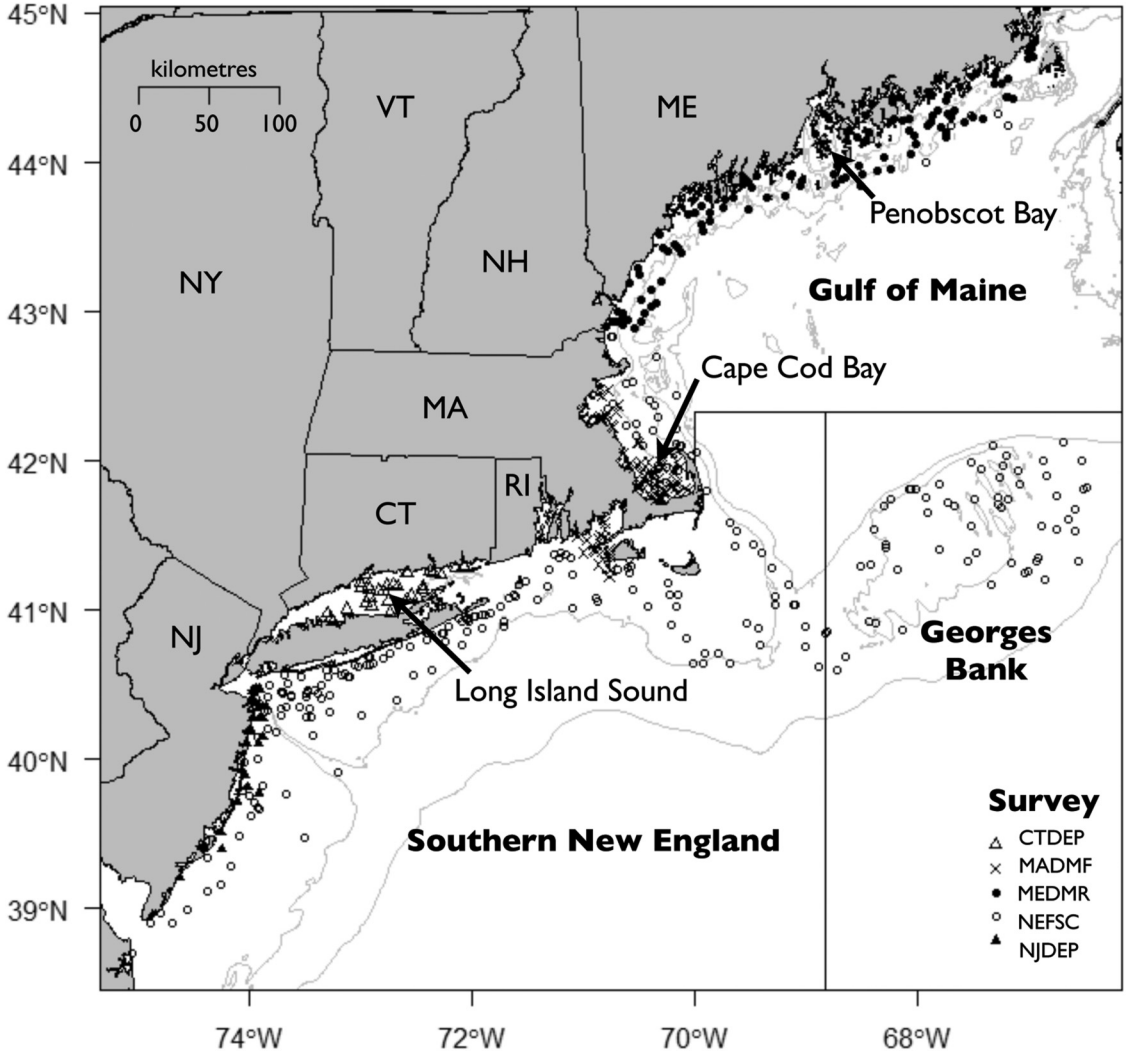

effects can be incorporated to reflect changes in the response variable as a function of both location and the covariates of interest. A spatially explicit version of the maturity models described above can be specified as

$$\text{logit}(\mu_{ij}) = \beta_0 + f_1(x_i, \text{Latitude}_j, \text{Longitude}_j) \quad (3)$$

where f_1 is a tensor product interaction of a one-dimensional smooth function for size or age i and a two-dimensional isotropic smooth for location j. The tensor product construction of this interaction term allows for maturity to be modeled as a smooth function of space and size or age over the study area while being invariant to their relative scaling (Wood 2006). Smoothness selection is determined using penalized iteratively reweighted least squares (Wood 2006); the estimated degrees of freedom (edf) associated with each smoother indicates the degree of nonlinearity of each resulting smooth function. The lower the edf, the more "linear" the estimated relationship, with an edf of 1 corresponding to a linear fit. The resulting model produces a smooth surface allowing the proportion of fish mature-at-size or -age to be estimated at any location within the study area; in other words, the model can be used to interpolate estimates, filling in gaps between sampled areas.

Nonlinear effects of environmental covariates, such as temperature, can be incorporated in a similar fashion. While temperature and location (whether in terms of latitude or longitude coordinates or stock) are by their nature correlated to some degree, by including both terms in the same model for maturity it is possible to estimate a general trend while accounting for localized effects (such as local adaptation; Butts and Litvak 2007). Full models used to investigate spatial variation and temperature effects on female winter flounder maturity were of the following structure:

$$\text{logit}(\mu_{ij}) = \beta_0 + f_1(x_i, \text{Latitude}_j, \text{Longitude}_j) + f_2(\text{Temperature}_j) \quad (4)$$

where $f_{1–2}$ indicate smooth functions of the covariates: f_1 is a tensor product interaction term as described above, and f_2 is a

Table 1. Classification of female winter flounder maturity based on gonad histology.

Maturity class	Gonad histology criteria
1. Immature	MAOS = perinucleolar Ovary wall thin; little connective tissue in the lamellae No POFs; few atretic oocytes
2. First-time maturing	MAOS = cortical alveolar or partially vitellogenic Ovary wall thin; little connective tissue in the lamellae No POFs; few atretic oocytes
3. Repeat developing	MAOS = partially vitellogenic Ovary wall thick; thick connective tissue in the lamellae No POFs
4. Developing	MAOS = fully vitellogenic
5. Ripening	MAOS = germinal vesicle migration
6. Ripe	MAOS = hydrated oocyte (i.e., within the follicle) No POFs
7. Ripe and running	MAOS = hydrated egg (i.e., outside the follicle) Fresh POFs present
8. Spent	MAOS = perinucleolar, cortical alveolar, or partially vitellogenic (residual, atretic eggs may remain) Ovary wall thick; thick connective tissue in the lamellae Many fresh or older–collapsed POFs present
9. Resting	MAOS = perinucleolar, cortical alveolar, or partially vitellogenic Ovary wall thick; thick connective tissue in the lamellae Older–collapsed POFs present
10. Skipped spawner	MAOS = perinucleolar (observed preceding or during spawning) Ovary wall thick; thick connective tissue in the lamellae No POFs

Note: Ovary walls with widths less than 150 μm were classified as thin; those greater than 150 μm were considered thick. The dashed line separates immature (1–2) from mature (3–10) classes. MAOS = most advanced oocyte stage; POF = postovulatory follicle. Criteria follow McBride et al. (2013).

smooth term for the mean annual bottom temperature at each location *j*. There are various types of smooth terms available; see Wood (2006) for mathematical details of smoother types. Herein we use a "spline on the sphere" smoother (Wahba 1981; Wood 2003) to represent maturity as a function of latitude and longitude because data were sampled over a large geographic area. The relationships among maturity and size or age and temperature were represented using thin plate regression splines (Wood 2006). Models not including an interaction between the spatial smoother and size or age and those estimating the effects of latitude, longitude, and temperature separately were also considered. All models were fit using the "mgcv" package (Wood 2006, 2011) in R (R Development Core Team 2013). In all cases, the gamma parameter, which penalizes models of increasing complexity, was set to 1.4 to reduce over-fitting (Wood 2006).

The effect of temperature on maturity was modeled in terms of the mean annual bottom temperature (estimated as described below) averaged over a standard "home range" surrounding the capture location. To account for fish movement, the maximum mean recapture distance of tagged fish from all stock regions (26.1 km; Howe and Coates 1975; Phelan 1992; Pereira et al. 1994; Fairchild et al. 2013) was used to estimate the area of probable locations occupied. Temperatures within the 2148 km^2 home range surrounding the collection location were then averaged to produce an estimate for each flounder. If the resulting home range of a particular fish overlapped the coast, only temperatures from coastal waters were used. While this simplifying assumption is likely more appropriate for some regions or contingents of fish than others (DeCelles and Cadrin 2010; Fairchild et al. 2013; Frisk et al. 2014), it was necessary given the absence of actual movement data; we were not able to reliably estimate movement patterns, and thus average ambient temperatures, for each fish over the course of the year. We initially also evaluated the effect of temperature variability using the estimated range in temperature experienced over the course of a year at each location, but this metric was collinear with the mean and provided essentially the same information (Pearson correlation coefficient = 0.94; Fig. S2[1]). Therefore, only results based on the mean annual temperature are presented herein.

Temperature estimation

Bottom temperature data were obtained from water column profiles collected during NEFSC surveys of the northeast US continental shelf (http://www.nefsc.noaa.gov/epd/ocean/MainPage/ioos.html). For Long Island Sound, data were acquired from the CTDEP Ambient Water Quality Monitoring Program (http://www.lisicos.uconn.edu/dep_portal.php). Temperatures in the region have increased over time (Friedland and Hare 2007; Nye et al. 2009); therefore, we limited the analysis to data collected during the lifespans of the flounder sampled (1996–2012; NEFSC: n = 25 700; CTDEP: n = 3580).

Bottom temperature data did not exist for each location within the study area on every day of the year, but the available data did provide extensive geographic coverage of the area over which fish were sampled (between 38°N–45°N and 65°W–75°W; Fig. 2). Daily values were interpolated by fitting a GAM to the available temperature data as a function of location (i.e., latitude, longitude) and day of the year (Julian day). Although temperature varies both annually and at finer spatial scales, our goal was to model temperature at a similar temporal and spatial scale as maturity (i.e., a multiyear process occurring over the area occupied by an individual fish). Therefore, more complex physical factors that may affect temperature (e.g., oceanic fronts, depth, upwelling indices, advection, destratification; Knauss 1997) were not considered.

Preliminary analyses indicated that the data were best represented with a Gaussian error distribution with an identity link; therefore, the expected temperature on day i at location j was modeled as

$$E(\text{Temperature}_{ij}) = \beta_0 + f_3(\text{Day}_i, \text{Latitude}_j, \text{Longitude}_j) \quad (5)$$

where f_3 indicates a tensor product of a one-dimensional smooth term for day of the year (Julian day) and a two-dimensional isotropic spline on the sphere smooth for location. The effect of day was

Fig. 2. Mean annual bottom temperatures (°C) predicted over the study area (*a*). Estimates were obtained as the mean of daily values estimated for each location based on a generalized additive model. Contour lines delineate regions with similar estimates. The circle beneath the temperature legend indicates the size of the home range over which mean temperature was estimated for each fish. The inset shows the distribution of collected temperature data that were used to fit the model. Stars indicate the specific locations for which annual temperature curves are presented to illustrate regional differences (*b*). The shaded region in panel (*b*) indicates the preferred temperature range for winter flounder (Pereira et al. 1999). The mean annual bottom temperature for each location is presented in parentheses in the legend.

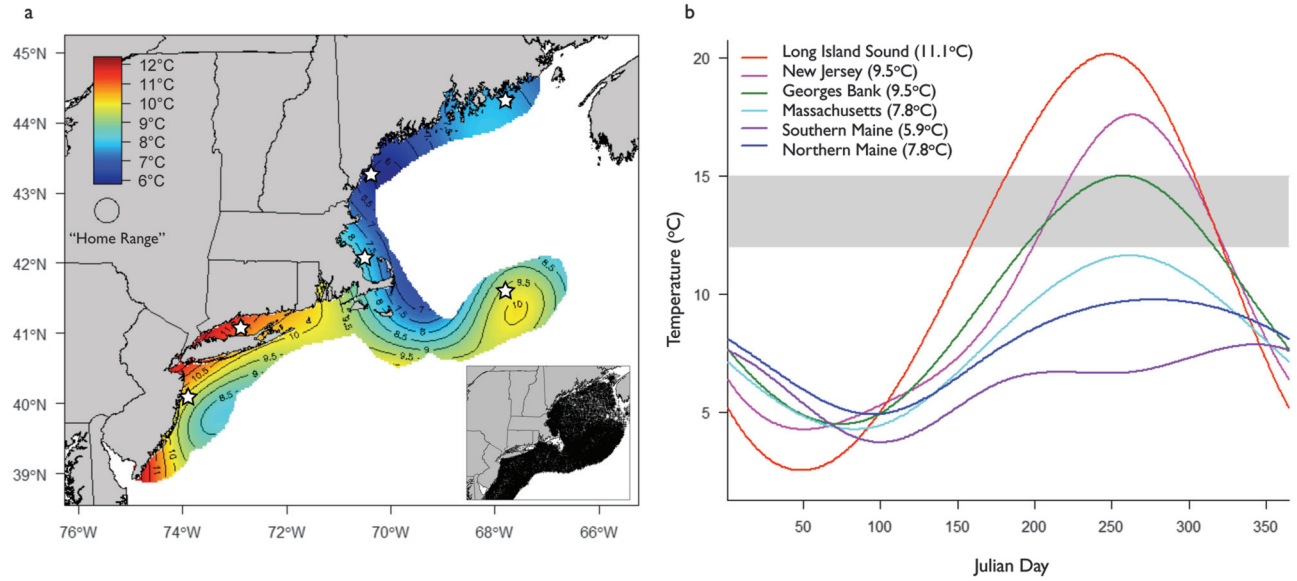

Table 2. Relative goodness of fit for candidate bottom temperature models.

Model	edf	GCV	Deviance explained	AIC	Δ_i
f(Day, Latitude, Longitude)	98.66	3.66	0.81	120 691	0
f(Day) + *f*(Latitude, Longitude)	57.55	8.24	0.57	144 456	23 765
f(Day) + *f*(Latitude) + *f*(Longitude)	25.99	9.76	0.49	149 414	28 723
f(Day)	8.94	12.59	0.34	156 864	36 173
f(Latitude, Longitude)	49.24	15.16	0.20	162 260	41 569
f(Latitude) + *f*(Longitude)	16.20	16.58	0.13	164 905	44 214

Note: Models are ranked from best- to worst-fitting. Day = Julian day of the year; Latitude = latitude in decimal degrees; Longitude = longitude in decimal degrees; edf = total model estimated degrees of freedom; GCV = generalized cross-validation score; AIC = Akaike information criterion; Δ_i = AIC difference. *f* indicate smooth terms; see text for specifics on the types of smooth functions used for each covariate.

represented with a cyclic cubic regression spline to ensure continuity between the first and last day of the year (Wood 2006). Simpler models nested within the above equation (without the interaction term between location and day as well as those incorporating the effects of latitude and longitude separately) were also considered. All models were fit using the "mgcv" package (Wood 2006, 2011) in R (R Development Core Team 2013). In all cases, the gamma parameter, which penalizes models of increasing complexity, was set to 1.4 to reduce over-fitting (Wood 2006). All models considered are listed in Table 2. Based on the best-fitting model, daily values predicted over the study area were used to estimate the mean annual bottom temperature as well as the mean range of temperatures experienced at any given location.

Model selection and evaluation

Model fit was evaluated based on the Akaike information criterion (AIC; Akaike 1973; Burnham and Anderson 2002), the generalized cross-validation score (GCV; for models assuming a Gaussian error distribution) or unbiased risk estimator (UBRE; for models assuming a binomial error distribution), and the proportion of the deviance explained (Wood 2006). The GCV and UBRE are smoothing parameter estimation criteria. The UBRE minimizes the expected mean square error when the scale parameter is assumed known; the GCV minimizes prediction error based on a "leave-one-out" cross-validation scheme when the scale parameter is unknown (Wood 2006). Interaction and individual terms were retained in the model if their inclusion resulted in lower AIC and GCV or UBRE scores and explained a higher proportion of the deviance. The AIC difference (Δ_i) of each model was calculated based on the lowest observed AIC value (AIC_{min}) as $\Delta_i = AIC_i - AIC_{min}$; models with $\Delta_i < 2$ were considered indistinguishable in terms of fit (Burnham and Anderson 2002). Residual plots were examined to confirm model assumptions.

Prediction of maturity throughout the study area

The geographic area for parameter estimation was bounded roughly by sampling locations where both immature and mature specimens were collected to ensure model convergence and avoid extrapolation into unsampled areas (Augustin et al. 1998). The resulting models can be used to predict estimates at any spatial resolution within the study area; we chose to grid the study area into 10 000 grid cells (0.03° × 0.03°) to produce high-resolution maps for ease of interpretation. Based on the selected maturity models, the median size- and age-at-maturity (TL_{50} and A_{50}, respectively) were estimated for each grid cell and plotted over the study area to generate a smooth maturity surface. Standard errors of the estimates were also plotted to identify regions with poor data coverage or model convergence issues.

Spatial patterns in maturity schedules

Subareas with similar maturity schedules were determined using a clustering algorithm developed by Ruß and Kruse (2011) for the analogous task of delineating agricultural management zones based on soil characteristics. The approach takes advantage of the autocorrelation present in geo-referenced data to produce spatially coherent clusters. Here we briefly describe the algorithm, which, as far as we are aware, has not yet been applied to a fisheries problem.

The area of interest is initially partitioned by overlaying a grid and extracting the mean values for each cell. Grid cells are then merged consecutively into clusters using a hierarchical agglomerative clustering approach assuming an average linkage. The algorithm produces clusters of grid cells with similar attributes, which are sequentially merged based on similarity to adjacent and nonadjacent clusters. The sequence proceeds from the initial number of gridded cells to a final, single cluster. Initially, only spatially adjacent grid cells or clusters can be merged; all "neighboring" cells are identified, and those with the smallest attribute distance between them in terms of the selected dissimilarity metric (usually Euclidean distance) are combined. In later steps, both adjacent and nonadjacent clusters can be merged. When the ratio of the median distance between nonadjacent and adjacent clusters falls below a designated contiguity ratio threshold, cp, the formation of noncontiguous clusters can occur. The results can be used to explore the spatial extent of clusters at varying degrees of similarity; however, the approach does not indicate whether any one solution (number of clusters) has more support than another.

We applied the clustering algorithm as presented in Ruß (2012) for R (R Development Core Team 2013) as follows. The interpolated maturity surfaces based on the best fitting size- and age-at-maturity models were divided into 1000 grid cells (0.10° × 0.10° resolution). The TL_{50} and A_{50} predicted for each cell were scaled and centered to give each predictor equal weight in the analysis. Euclidean distance was used as the dissimilarity measure, and the cp was set at 1.5, requiring that the median distance between nonadjacent clusters be less than 1.5 times the median distance between adjacent clusters before noncontiguous clusters could be formed. This setting was selected to balance spatial contiguity with cluster similarity (Ruß 2012). Because we did not have sufficient data to suggest a threshold for biologically meaningful distances between clusters, we examined the results of the last nine clustering steps (k = 2–10) as a means of exploring underlying spatial structure at a similar scale as current management structure (three stocks). Finer scale clustering had limited practical applicability.

Results

Fish collected ranged in size from 85 to 600 mm TL. Comparable numbers of immature (n = 751) and mature flounder (n = 863) were sampled, and there was a large degree of overlap in the size and age of immature and mature female winter flounder. The largest immature female (381 mm TL) was collected in Cape Cod Bay; the smallest mature individual was 152 mm TL and collected off the coast of northern Maine. Age estimates ranged from 1 to 7 and from 2 to 14 years for immature and mature fish, respectively. The two oldest immature females (age 7) were collected off the coast of New Hampshire and southern Maine. Age 2 mature fish (n = 49) occurred over a large portion of the study area and were collected from coastal waters off New Jersey (n = 28), New York (n = 1), Massachusetts (n = 3), and northern Maine (n = 16), as well as offshore on GB (n = 1).

Temperature estimation

Bottom temperatures were best represented by the model including the location–day smoother (Table 2), suggesting difference in the shape of the annual temperature curve over the study area. Dropping the interaction term between location and day greatly reduced fit ($\Delta_i \geq 23\,765$ in all cases). Day explained more of the variability in temperature (deviance explained = 0.34) than the location smoother alone (deviance explained = 0.20). Models representing spatial variation in temperature using the spatial smoother performed better than those including the effects of latitude and longitude separately (Table 2).

Predicted mean bottom temperatures ranged from 5.8 to 12.4 °C over the study area (Fig. 2*a*). Those estimated for individual fish spanned this range (as low as 5.9 °C for fish collected off the coast of southern Maine and as high as 12.4 °C for those collected off southern New Jersey). The predicted intra-annual range in temperature at any given location was lowest in the GOM (3.4 °C) and highest for Long Island Sound (22.1 °C). Model standard errors were highest for the GOM, particularly for coastal areas where the available bottom temperature data were sparse (Fig. S3[1]). Predicted temperatures and the shapes and magnitude of the annual cycle at specific locations (Fig. 2*b*) corresponded well with area-specific estimates produced using a three-part harmonic curve-fitting procedure (Mountain and Holzwarth 1989), indicating that the selected GAM sufficiently captured local seasonal changes in temperature across the entire study area.

Maturity models

Variation in size- and age-at-maturity was best described by spatially explicit GAMs (Table 3). Dropping the interaction term between location and TL or age reduced fit in both cases (TL: $\Delta_i \geq 18$; age: $\Delta_i \geq 30$). All models incorporating location as a function of geographic coordinates performed better than models incorporating stock area as a proxy for spatial structure (TL: $\Delta_i \geq 142$; age: $\Delta_i \geq 136$). The incorporation of mean annual temperature improved both maturity models over those based only on size or age and stock area (Table 3). However, adding temperature to models including geographic coordinates did not improve fit or explain additional variability (Table 3), suggesting that the effect of location better encompassed environmental and other conditions contributing to maturity.

Model-based interpolation of TL_{50} and A_{50} estimates over the study area suggested a high degree of spatial variation between as well as within the three US stock areas (Table 4; Fig. 3). Median size-at-maturity estimates ranged from 172 to 356 mm TL over the study region. The smallest TL_{50} was estimated for winter flounder in the northern GOM, with fish on GB maturing at the largest sizes (Fig. 3*a*). Age-at-maturity estimates generally followed a south-to-north pattern; the lowest A_{50} was estimated for fish off of New Jersey (<2.5 years) and the highest for the GOM off southern Maine and north of Penobscot Bay (>4.5 years; Fig. 3*b*). The standard error of the estimate for both TL_{50} and A_{50} was largest for coastal waters off southern New Jersey and the eastern edge of GB, where fewer fish were collected (Fig. S4[1]).

Spatial patterns in maturity schedules

Spatially constrained cluster analysis of TL_{50} and A_{50} suggested greater variation within than between existing stock areas, particularly in the GOM (Fig. 4). The median distance between nonadjacent and adjacent clusters fell below the spatial contiguity constraint (cp < 1.5) when seven clusters remained (Fig. 4*d*), allowing for the formation of noncontiguous clusters. However, subsequent steps did not produce noncontiguous clusters (Figs. 4*e*–4*i*). The choice of cp was relatively robust and did not affect the general interpretation of the results. Setting cp below 1.5 did not change the sequence of clusters formed; setting it to 2.0 shifted the boundary of the cluster off Massachusetts slightly northward (Fig. S5[1]).

In terms of maturity, GB was more similar to the northernmost portion of the SNE than the subclusters identified in both the SNE (n = 3) and GOM (n = 6) were to each other (Figs. 4*a*, 4*b*). Distinct subregions were apparent in both SNE and GOM (Figs. 4*b*–4*h*). The

Table 3. Relative goodness of fit for candidate size- (n = 1614) and age-at-maturity (n = 1443) models.

Model	edf	UBRE	Deviance explained	AIC	Δ_i
Size-at-maturity models					
f(TL, Latitude, Longitude) + *f*(Temperature)	23.63	−0.36	0.56	1019	0
f(TL, Latitude, Longitude)	19.48	−0.36	0.56	1021	2
TL + *f*(Latitude, Longitude)	17.28	−0.35	0.55	1038	18
TL + *f*(Latitude, Longitude) + *f*(Temperature)	17.58	−0.35	0.55	1038	19
TL + *f*(Latitude) + *f*(Longitude)	11.52	−0.34	0.54	1053	33
TL + *f*(Latitude) + *f*(Longitude) + *f*(Temperature)	10.57	−0.34	0.54	1055	36
TL × Stock + *f*(Temperature)	9.61	−0.28	0.49	1161	142
TL × Stock	6.00	−0.27	0.48	1172	152
TL + Stock + *f*(Temperature)	7.08	−0.23	0.45	1240	220
TL + *f*(Temperature)	8.54	−0.22	0.45	1248	229
TL + Stock	4.00	−0.22	0.44	1253	233
TL	2.00	−0.18	0.41	1326	307
Age-at-maturity models					
f(Age, Latitude, Longitude)	21.23	−0.27	0.50	1037	0
f(Age, Latitude, Longitude) + *f*(Temperature)	21.56	−0.27	0.50	1038	1
Age + *f*(Latitude, Longitude)	21.46	−0.25	0.49	1067	30
Age + *f*(Latitude, Longitude) + *f*(Temperature)	22.01	−0.25	0.49	1068	31
Age + *f*(Latitude) + *f*(Longitude)	13.97	−0.23	0.46	1099	63
Age + *f*(Latitude) + *f*(Longitude) + *f*(Temperature)	15.01	−0.23	0.46	1101	64
Age × Stock + *f*(Temperature)	11.41	−0.19	0.42	1172	136
Age + *f*(Temperature)	3.00	−0.17	0.40	1195	158
Age + Stock + *f*(Temperature)	9.53	−0.17	0.41	1195	158
Age × Stock	6.00	−0.15	0.39	1222	185
Age + Stock	4.00	−0.14	0.38	1247	210
Age	2.00	−0.03	0.30	1396	359

Note: Models are ranked from best- to worst-fitting. TL = total length (in mm); Latitude = latitude in decimal degrees; Longitude = longitude in decimal degrees; Temperature = mean annual bottom temperature; edf = total model estimated degrees of freedom; UBRE = unbiased risk estimator; AIC = Akaike information criterion; Δ_i = AIC difference. *f* indicates a smooth function; see text for specifics on the types of smooth functions used for each covariate. A multiplication symbol (×) indicates an interaction term.

Table 4. Estimated median size- and age-at-maturity for each of the three United States' winter flounder stock areas as predicted by a generalized linear model (GLM) incorporating stock area and a spatially explicit generalized additive model (GAM).

	Total length (mm)			Age (years)		
	GLM	GAM		GLM	GAM	
Stock	Median	Median	Range	Median	Median	Range
Southern New England (n = 592)	298	305	252–336	2.6	3.1	1.4–3.6
Georges Bank (n = 88)	344	342	328–356	3.1	3.1	3.0–3.3
Gulf of Maine (n = 934)	258	252	172–294	3.9	3.9	2.3–4.6

area surrounding Penobscot Bay, Maine, in particular, stood out; this cluster exhibited greater dissimilarity to the rest of the GOM stock than the SNE and GB stocks did to each other (Fig. 4*h*). In terms of the three existing stock areas, the GOM was the most distinct from the other two (Fig. 4*i*).

Discussion

By approaching the estimation of maturity in a GAM framework, we were able to model variation in female winter flounder maturity throughout the species' distribution in US waters. The results aligned well with more general patterns previously reported for discrete stock regions (McBride et al. 2013) but recognized intrastock variation on a much finer scale. Not surprisingly, maturity models explicitly incorporating spatial structure explained more variation than the "traditional" approach of aggregating data according to stock boundaries. The approach outlined here provides a method for identifying areas with different vital rates without the need to presume subjective boundaries, making it informative as part of an interdisciplinary approach to stock identification (McBride 2014).

In contrast with the traditional maturity models applied, GAM-based models provided insight into complex spatial patterns at a resolution that more likely captures the underlying mechanisms driving observed variation. The patterns of TL_{50} and A_{50} estimated over the study area support the three current US stock areas but also indicate substantial variation within both the GOM and SNE stocks (Figs. 3, 4; Table 4). These results suggest that GB is the most homogeneous of the three existing stock areas; the range of TL_{50} estimates varied by less than 28 mm and A_{50} by only 0.3 years within GB. In contrast, median size-at-maturity estimates differed by 84 and 122 mm TL within the SNE and GOM stocks, respectively. Age-at-maturity estimates also varied by more than 2 years within each region (Table 4), which is approximately double the difference reported among substock areas by McBride et al. (2013). Within the SNE stock area, TL_{50} and A_{50} generally increased with latitude. Trends in the GOM were not so clear-cut; the area surrounding Penobscot Bay, Maine, where fish matured at smaller sizes and ages, interrupted the general trend of decreasing TL_{50} and increasing A_{50} with latitude. The standard errors of the estimated size- and age-at-maturity indicated poor fit in some areas at

Fig. 3. Median size- (*a*) and age-at-maturity (*b*) of female winter flounder from US waters as predicted over the study area using generalized additive models incorporating spatial structure. Boundaries for the three stock areas are indicated by black lines. Contour lines delineate regions with similar estimates. Values predicted for each stock area using a generalized linear model are presented outside of the prediction area.

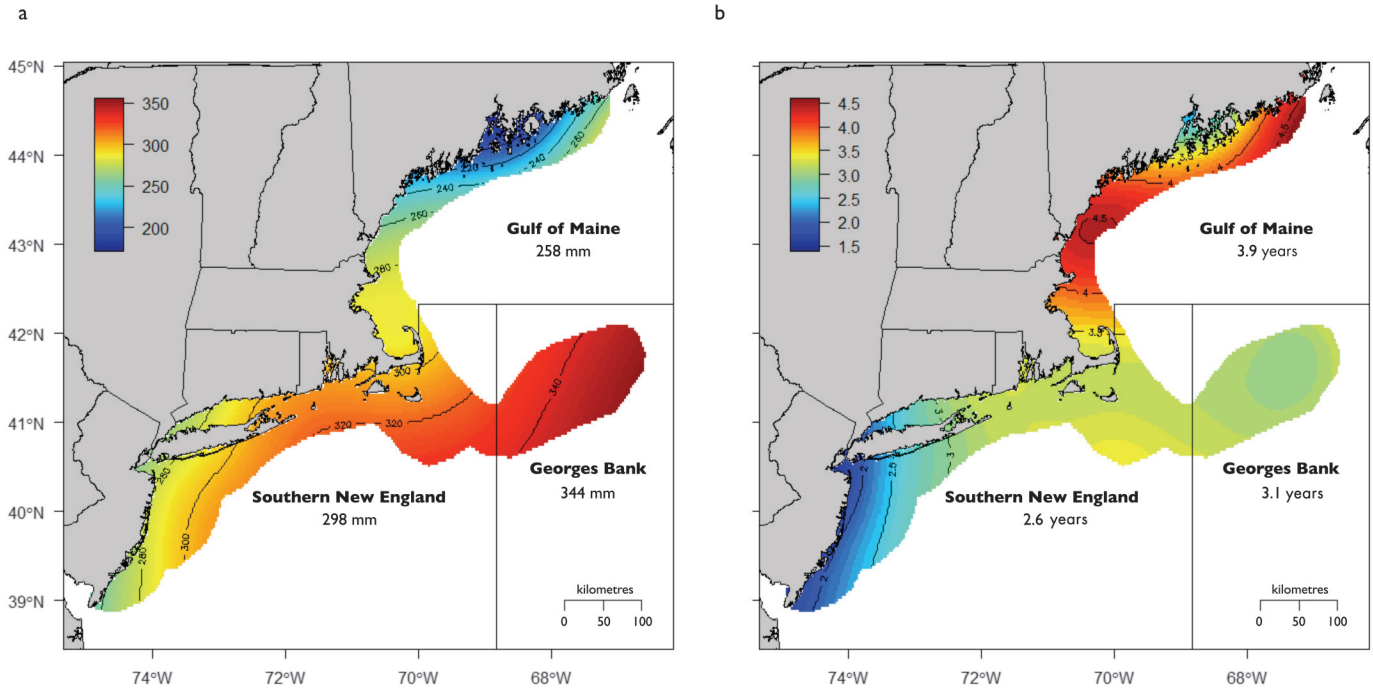

the edge of species' exploitable range where the numbers of fish collected were relatively low (i.e., southern New Jersey and the southeastern edge of GB; Fig. S4[1]).

Effect of temperature on maturity schedules

We postulated that mean temperature would provide a sufficient but relatively simple metric to explain observed variation in maturity, but as Brander (1995) noted, the hypothesis that temperature is the only factor governing growth, and hence size at maturation, is "an absurd hypothesis at best." The GAM-based predictions of daily bottom temperatures accounted for local variation well (explaining 81% of the observed variation in temperature; Table 2) and agreed with regional estimates previously produced using a three-part harmonic curve-fitting procedure (Mountain and Holzwarth 1989). Although the incorporation of mean temperature did improve the fit of maturity models based on size or age and stock area, spatially explicit models explained a much larger proportion of the observed variability in maturity than temperature alone (Table 3). This was not surprising; location encompasses other factors not accounted for in the model (among them habitat variability, food availability, or fine-scale variation in actual, rather than estimated, temperature), and maturation is a multiyear integration of a series of processes that vary spatially. However, models incorporating temperature data at a higher resolution (in terms of both time and space) might explain a larger portion of the variability observed (Brander 1995; Manderson et al. 2011). While remote-sensing technology has made high-resolution temperature data broadly available for surface waters, the challenge of linking conditions at the surface to the benthos remains (Manderson et al. 2011).

Several studies have suggested that mean regional temperatures are poor proxies for a fish's thermal environment. Rather, the actual temperature of the water surrounding an individual fish may be required to accurately evaluate the effects of temperature on life history (Brander 1995). While fish on GB remain in essentially the same habitat, inshore stocks inhabit distinctly different habitats during different life stages, with fish in the GOM and SNE presumably residing in estuaries their first year of life (Pereira et al. 1999). Even among coastal stocks, contingents exhibiting divergent movement patterns exist (DeCelles and Cadrin 2010; Fairchild et al. 2013; Frisk et al. 2014). Therefore, temperatures experienced by individuals from the same general area may vary substantially. Flounder inhabiting inshore areas also migrate in response to temperature (Howe and Coates 1975), confounding the estimation of mean temperatures. It is also probable that temperature during discrete periods of the year or life cycle is more important than the average environment experienced by an individual (Tobin and Wright 2011). Ontogenetic shifts in thermal tolerance further complicate interpretation of predicted relationships (Johnson et al. 2013).

Available tagging studies, while limited, do suggest that winter flounder in SNE tend to migrate larger distances than those in the GOM and GB stock areas (Howe and Coates 1975; Phelan 1992; Fairchild et al. 2013); however, sufficient data were not available to reliably estimate movement patterns to generate region-specific home ranges. While the mean home range we applied for all stock areas is likely an overestimate for fish in the GOM, annual temperature curves and estimates for that region exhibited less variation than in the SNE and GB stock areas (Fig. 2*b*). Therefore, including a larger radius than likely in the GOM would not affect estimates as much as assuming too small a home range in SNE. This approach does not eliminate the problem that the mean temperature of the area surrounding a fish's collection site is a poor estimate of ambient temperatures experienced by a mobile creature over the course of a year or its lifetime. It will likely take individual-based telemetry studies employing temperature loggers to adequately estimate the thermal habitat of fish in different regions.

Nevertheless, winter flounder do not generally undertake extensive north–south migrations (Howe and Coates 1975), making the use of mean annual temperature a reasonable approximation to an individual's thermal habitat. Several recent studies have estimated the thermal environment of fish in terms of growing

Fig. 4. Final nine iterations of a spatially constrained, hierarchical agglomerative cluster analysis for female winter flounder size- and age-at-maturity in US waters. Mean values (age in years, total length in mm) for each cluster are indicated. The spatial constraint was switched off in panel (*d*); however, noncontiguous clusters were not formed in any of the subsequent steps (*e*–*i*).

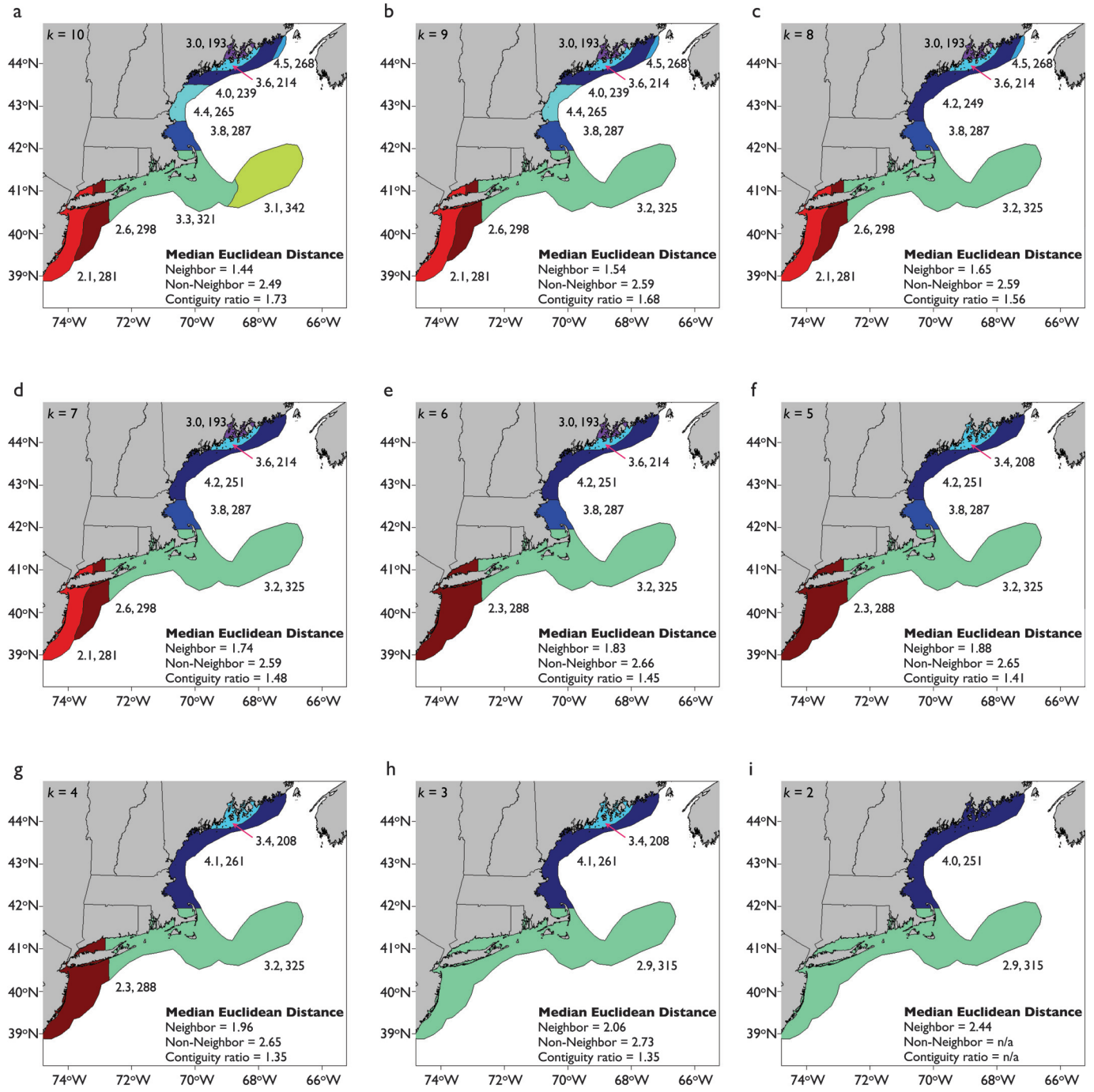

degree-days, or the accumulated thermal growth potential of an individual over its lifetime (Neuheimer and Taggart 2007). The applicability of this metric has been demonstrated in terms of explaining growth and maturity in laboratory and wild fish populations, although the relationship appears to break down near the extremes of the temperature range (Neuheimer and Taggart 2007). Studies investigating the physiological effects of cold or heat stress on larval, young of the year, and juvenile winter flounder exist (Pereira et al. 1999), but reliable information for all stages of the life cycle is not available. As such, trying to estimate an age-based, individual-specific thermal index for a species exhibiting ontogenetic shifts in habitat as well as thermal tolerance was unrealistic (Smart et al. 2012). Therefore, we believe our approach of using GAMs and letting the available data determine the structure of the relationship between maturity and temperature was the most robust, informative approach in terms of the data available.

Other factors undoubtedly complicate the identification and interpretation of the relationship between temperature and maturity. Winter flounder exhibit some degree of spawning site fidelity (Howe and Coates 1975; Phelan 1992; Fairchild et al. 2013), and dispersal of benthic eggs from estuarine or coastal spawning

areas is limited (Pereira et al. 1999; DeCelles and Cadrin 2011), indicating a likelihood of locally adapted populations (e.g., differences in gene copy number and arrangement of antifreeze proteins; Hayes et al. 1991). Given the broad latitudinal distribution of the species and limited movements of immature individuals, it is possible that fish within a region or subregion may be better adapted to local thermal environments (Everich and González 1977) or have different inherent capacities for growth (Butts and Litvak 2007; Kerr and Secor 2009; Bolton-Warberg et al. 2013), obscuring the overall relationship between temperature and growth or maturation.

While temperature is certainly one of the most important factors affecting an organism and its physiological processes, food availability and quality also undoubtedly play a major role in driving life history variability. Productivity along winter flounder's US range is spatially variable, as indicated by satellite-derived measures of chlorophyll (Ecosystem Assessment Program 2009), although translation of productivity at the surface to the food available for benthic fishes is difficult (Manderson et al. 2011). In some regions of the GOM, winter flounder cease feeding in the winter during periods of prolonged low temperatures (Pereira et al. 1999; Plante et al. 2005), while in SNE winter temperatures likely do not limit feeding (Wuenschel et al. 2009).

In addition to the genetic and environmental effects mentioned above, exploitation-mediated shifts in regional life histories cannot be overlooked. All three stocks have experienced periods of overfishing over the past several decades but have exhibited different levels of recovery (Northeast Fisheries Science Center 2011). Therefore, size-selective mortality or density-dependent effects may have played a role in shaping the current pattern of life history variability in the species (McBride 2014). Commercial landings in all three stock areas peaked in the 1970s and 1980s and declined thereafter. The most recent stock assessment (Northeast Fisheries Science Center 2011) determined that overfishing was no longer occurring in all three stocks, but the overfished status (whether current biomass estimates are below the minimum threshold value) differed. The assessment indicated that the GB stock has not been overfished since 1996, but that the SNE stock remains overfished. The available data were not sufficient to determine whether or not the GOM stock was overfished. Future studies should seek to incorporate estimates of exploitation rates or relative population densities, although it may be difficult to disentangle such effects given the long exploitation history of the species (DeCelles and Cadrin 2011).

Management implications

Models explicitly incorporating spatial structure performed better than those based on current management areas or temperature (for the reasons detailed above), but the very lack of predefined boundaries that made the approach intuitively appealing produced the following challenge: how should we interpret the results in a manner meaningful for fisheries managers? It is not economically or logistically feasible to incorporate fine-scale spatial variability into assessments. In a similar vein to the approach we used (Ruß 2012), Cope and Punt (2009) used a two-step, *k*-medoids clustering approach to identify both the number and boundaries of "true" stock areas based on abundance indices as well as abundance index uncertainty. Their approach is generally applicable to the identification of natural boundaries and could be extended to life history data to identify discrete population subunits. Here, our goal was not to identify specific groupings in the data, but rather to explore varying degrees of difference in maturity estimates over the study area via a hierarchical clustering approach. As such, our results should not be considered a definitive assessment of stock structure and do not represent a "stand-alone" approach to stock identification, nor do they indicate a need to restructure current stocks.

The results corroborate previous evidence that substantial phenotypic variation may occur within the SNE stock area (McBride et al. 2013). Fish from the southern portion of the SNE stock area mature at smaller sizes and younger ages; estimates for the northern portion are more similar to those for GB. Not surprisingly, the observed break separating the SNE stock at Long Island Sound (Fig. 4*g*) aligns well with historic stock boundaries separating the region into two stock areas prior to the 1990s, when the stocks were combined based on evidence of substantial mixing during the commercial season as well as similarities in life histories (DeCelles and Cadrin 2011; Northeast Fisheries Science Center 2011). In contrast with the difference apparent between flounder west of Long Island Sound and the rest of the SNE (which may represent a biologically meaningful shift in vital rates), the break apparent off New Jersey (Fig. 4*d*) parallels the coast and is likely more reflective of differences in the inshore–offshore distribution of spawning and immature fish during the period of sample collection. Similarly, Cope and Punt (2009) found that their two-step clustering approach identified units reflective of spatially structured life history stages in Pacific cod (*Gadus macrocephalus*).

Interestingly, winter flounder on GB, which are generally regarded to be distinct from coastal stocks in terms of size and growth (Pereira et al. 1999), were more similar in terms of maturity to the northernmost portion of the SNE stock than any of the SNE or GOM substock clusters were to each other (Figs. 4*a*, 4*b*). A recent genetic analysis also reported limited genetic divergence between GB winter flounder and those collected south of Cape Cod, Massachusetts (Wirgin et al. 2014). However, it is important to note that the similarity between maturity estimates for GB and the northern portion of SNE may be due in part to model structure and the relative sparseness of the maturity data in those areas, as there is limited evidence of migration between the two regions (Howe and Coates 1975).

Winter flounder stock structure within the GOM has been the least well described of the three US stock units, but interchange of individuals in this area has been assumed sufficient to manage the area as one stock (DeCelles and Cadrin 2011). Our results suggest discernible substock regions (in terms of maturity) in the southern and northern GOM (Fig. 4), with a discrete area centered on Penobscot Bay, Maine, where winter flounder mature at younger ages and smaller sizes. Studies investigating movement patterns, seasonal residency, and contingent structure should be conducted to verify and further explore the heterogeneity among stock units identified herein.

Data permitting, the approach we have used can be broadly applied to investigate fine-scale variation in maturity, as well as processes that may influence it, over large or small spatial scales. The results for female winter flounder suggest a high degree of variation in maturity at finer scales than the current boundaries of the two inshore stocks, which may warrant further investigation. It is important to note that the analysis did not consider spatial patterns of stock abundance, fishing effort, or centers of biomass, all of which limit interpretation with respect to stock productivity. The estimated TL_{50} or A_{50} for a given area may be different from the rest of the stock management unit, but this difference may not have a great effect on stock productivity if a low percentage of the harvestable population resides there. The inherent weighting present in traditional maturity models (where locations with greater population densities are typically represented by more samples and hence contribute more to overall stock estimates) provides estimates at the proper scale for defined stock units. However, the approach presented herein allows for exploration of fine-scale variability underlying estimates for broad regions, which can be informative as part of an interdisciplinary approach to stock identification. A logical next step would involve the construction of spatially explicit population models to evaluate how such fine-scale variability may impact stock produc-

tivity, as well as how its effects may change in response to fishing mortality and environmental conditions.

Acknowledgements

The authors thank E. Towle, Y. Press, and D. McElroy for their help with all aspects of this project. They are also grateful to survey staff from the Ecosystems Survey Branch, Northeast Fisheries Science Center; the New Jersey Department of Environmental Protection (A. Mazzarella, H. Carberry, L. Berry, R. Ford, and the crew of the R/V *Seawolf*); the Massachusetts Division of Marine Fisheries (M. Szymanski, V. Manfredi, M. Camisa, and the crew of the R/V *Gloria Michelle*); the Maine Department of Marine Resources (S. Sherman, K. Stepanek, C. King, and the crew of the F/V *Robert Michael*); and the Connecticut Department of Environmental Protection (K. Gottschall and D. Pacileo). G. Thornton (NEFSC), J. Burnett (NEFSC), K. Stepanek (MEDMR), and S. Sherman (MEDMR) aged the specimens. P. Fratantoni, J. Manning, and B. Shank (NEFSC) provided advice regarding the bottom temperature data and analysis. M. Terceiro and P. Nitschke provided information from stock assessments as well as valuable insight into the interpretation of results. Mass Histology Service, Inc. processed all gonad tissue. The views expressed herein are those of the authors and do not necessarily reflect those of the National Marine Fisheries Service. Funding for this research was provided by the NMFS Habitat Assessment Improvement Team.

References

Akaike, H. 1973. Information theory as an extension of the maximum likelihood principle. *In* Second international symposium on information theory. *Edited by* B.N. Petrov and F. Csaki. Akademiai Kiado, Budapest, Hungary. pp. 267–281.

Augustin, N.H., Borchers, D.L., Clarke, E.D., Buckland, S.T., and Walsh, M. 1998. Spatiotemporal modelling for the annual egg production method of stock assessment using generalized additive models. Can. J. Fish. Aquat. Sci. **55**(12): 2608–2621. doi:10.1139/f98-143.

Augustin, N.H., Trenkel, V.M., Wood, S.N., and Lorance, P. 2013. Space–time modelling of blue ling for fisheries stock management. Environmetrics, **24**: 109–119. doi:10.1002/env.2196.

Bolton-Warberg, M., O'Keeffe, D., and FitzGerald, R.D. 2013. Exploring the temperature optima and growth rates of Atlantic cod at the south-easterly limit of its range. Aquacult. Res. 1–9. doi:10.1111/are.12215.

Brander, K.M. 1995. The effect of temperature on growth of Atlantic cod (*Gadus morhua* L.). ICES J. Mar. Sci. **52**: 1–10. doi:10.1016/1054-3139(95)80010-7.

Burnham, K.P., and Anderson, D.R. 2002. Model selection and multimodel inference: a practical information-theoretic approach. Springer, New York.

Butts, I.A.E., and Litvak, M.K. 2007. Stock and parental effects on embryonic and early larval development of winter flounder *Pseudopleuronectes americanus* (Walbaum). J. Fish Biol. **70**: 1070–1087. doi:10.1111/j.1095-8649.2007.01369.x.

Byrne, D. 1994. Stock assessment of New Jersey's nearshore recreational fisheries resources. *In* Proceedings of the Workshop on the Collection and Use of Trawl Survey Data for Fisheries Management. *Edited by* T. Berger. Atlantic States Marine Fisheries Commission, Washington, D.C. pp. 36–42.

Chen, Y., Sherman, S., Wilson, C., Sowles, J., and Kanaiwa, M. 2006. A comparison of two fishery-independent survey programs used to define the population structure of American lobster (*Homarus americanus*) in the Gulf of Maine. Fish. Bull. **104**: 247–255.

Cope, J.M., and Punt, A.E. 2009. Drawing the lines: resolving fishery management units with simple fisheries data. Can. J. Fish. Aquat. Sci. **66**(8): 1256–1273. doi:10.1139/F09-084.

DeCelles, G.R., and Cadrin, S.X. 2010. Movement patterns of winter flounder (*Pseudopleuronectes americanus*) in the southern Gulf of Maine: observations with the use of passive acoustic telemetry. Fish. Bull. **108**: 408–419.

DeCelles, G.R., and Cadrin, S.X. 2011. An interdisciplinary assessment of winter flounder (*Pseudopleuronectes americanus*) stock structure. J. Northwest Atl. Fish. Sci. **143**: 103–120. doi:10.2960/J.v43.m673.

Ecosystem Assessment Program. 2009. Ecosystem assessment report of the northeast U.S. continental shelf large marine ecosystem [online]. US Department of Commerce, Northeast Fish. Sci. Center Reference Document 09-11. Available from http://www.nefsc.noaa.gov/nefsc/publications/.

Everich, D., and González, J.G. 1977. Critical thermal maxima of two species of estuarine fish. Mar. Biol. **41**: 141–145. doi:10.1007/BF00394021.

Fairchild, E.A., Siceloff, L., Howell, W.H., Hoffman, B., and Armstrong, M.P. 2013. Coastal spawning by winter flounder and a reassessment of essential fish habitat in the Gulf of Maine. Fish. Res. **141**: 118–129. doi:10.1016/j.fishres.2012.05.007.

Friedland, K.D., and Hare, J.A. 2007. Long-term trends and regime shifts in sea surface temperature on the continental shelf of the northeast United States. Cont. Shelf Res. **27**: 2313–2328. doi:10.1016/j.csr.2007.06.001.

Frisk, M.G., Jordaan, A., and Miller, T.J. 2014. Moving beyond the current paradigm in marine population connectivity: are adults the missing link? Fish Fish. **15**(2): 242–254. doi:10.1111/faf.12014.

Hayes, P.H., Davies, P.L., and Fletcher, G.L. 1991. Population differences in antifreeze protein gene copy number and arrangement in winter flounder. Genome, **34**(1): 174–177. doi:10.1139/g91-027.

Howe, A.B., and Coates, P.G. 1975. Winter flounder movements, growth, and mortality off Massachusetts. Trans. Am. Fish. Soc. **104**: 13–29. doi:10.1577/1548-8659(1975)104<13:WFMGAM>2.0.CO;2.

Johnson, A.F., Jenkins, S.R., Hiddink, J.G., and Hinz, H. 2013. Linking temperate demersal fish species to habitat: scales, patterns and future directions. Fish Fish. **14**: 256–280. doi:10.1111/j.1467-2979.2012.00466.x.

Kennedy, V.S., and Steele, D.H. 1971. The winter flounder, *Pseudopleuronectes americanus*, in Long Pond, Conception Bay, Newfoundland. J. Fish. Res. Board Can. **28**(8): 1153–1165. doi:10.1139/f71-170.

Kerr, L.A., and Secor, D.H. 2009. Bioenergetic trajectories underlying partial migration in Patuxent River (Chesapeake Bay) white perch (*Morone americana*). Can. J. Fish. Aquat. Sci. **66**(4): 602–612. doi:10.1139/F09-027.

King, J.R., Camisa, M.J., and Manfredi, V.M. 2010. Massachusetts Division of Marine Fisheries trawl survey effort, lists of species recorded, and bottom temperature trends, 1978–2007. Massachusetts Division of Marine Fisheries Technical Report, TR-38.

Kingsolver, J.G. 2009. The well-temperatured biologist. Am. Nat. **174**(6): 755–768. doi:10.1086/648310. PMID:19857158.

Knauss, J.A. 1997. Introduction to physical oceanography. 2nd ed. Waveland Press, Long Grove, Ill.

Manderson, J., Palamara, L., Kohut, J., and Oliver, M.J. 2011. Ocean observatory data are useful for regional habitat modeling of species with different vertical habitat preferences. Mar. Ecol. Prog. Ser. **438**: 1–17. doi:10.3354/meps09308.

McBride, R.S. 2014. The continuing role of life history parameters to identify stock structure. *In* Stock identification methods: applications in fishery science. 2nd ed. *Edited by* S.X. Cadrin, L.A. Kerr, and S. Mariani. Elsevier Academic Press, San Diego, Calif. pp. 77–96.

McBride, R.S., Wuenschel, M.J., Nitschke, P., Thornton, G., and King, J.R. 2013. Latitudinal and stock-specific variation in size- and age-at-maturity of female winter flounder, *Pseudopleuronectes americanus*, as determined with gonad histology. J. Sea Res. **75**: 41–51. doi:10.1016/j.seares.2012.04.005.

Mountain, D.G., and Holzwarth, T.J. 1989. Surface and bottom temperature distribution for the northeast continental shelf. NOAA Technical Memorandum, NMFS-F/NEC-73.

NEFSC Vessel Calibration Working Group. 2007. Proposed vessel calibration for NOAA Ship *Henry B. Bigelow* [online]. US Department of Commerce, Northeast Fish. Sci. Center Reference Document 07-12. Available from http://www.nefsc.noaa.gov/nefsc/pub.

Neuheimer, A.B., and Taggart, C.T. 2007. The growing degree-day and fish size-at-age: the overlooked metric. Can. J. Fish. Aquat. Sci. **64**(2): 375–385. doi:10.1139/f07-003.

Northeast Fisheries Science Center. 2011. 52nd Northeast Regional Stock Assessment Workshop (52nd SAW) Assessment Summary Report [online]. US Department of Commerce, Northeast Fish. Sci. Center Reference Document 11-11. Available from http://www.nefsc.noaa.gov/nefsc/publications/.

Nye, J.A., Link, J.S., Hare, J.A., and Overholtz, W.J. 2009. Changing spatial distribution of fish stocks in relation to climate and population size on the Northeast United States continental shelf. Mar. Ecol. Prog. Ser. **393**: 111–129. doi:10.3354/meps08220.

Penttila, J., and Dery, L.M. 1988. Age determination methods for Northwest Atlantic species. NOAA Technical Report, NMFS 72.

Pereira, J.J., Goldberg, R., Clark, P.E., and Perry, D.M. 1994. Utilization of the Quinnipiac River and New Haven Harbor by winter flounder, *Pleuronectes americanus*, as a spawning area. Final Report to the New Haven Foundation, New Haven, Conn.

Pereira, J.J., Goldberg, R., Ziskowski, J.J., Berrien, P.L., Morse, W.W., and Johnson, D.L. 1999. Essential fish habitat source document: winter flounder, *Pseudopleuronectes americanus*, life history and habitat characteristics. NOAA Technical Memorandum, NMFS-NE-138.

Phelan, B.A. 1992. Winter flounder movements in the inner New York Bight. Trans. Am. Fish. Soc. **121**: 777–784. doi:10.1577/1548-8659(1992)121<0777:WFMITI>2.3.CO;2.

Plante, S., Audet, C., Lambert, Y., and de la Noüe, J. 2005. Alternative methods for measuring energy content in winter flounder. N. Am. J. Fish. Manage. **25**: 1–6. doi:10.1577/M03-104.1.

Press, Y.K., Wuenschel, M.J., and McBride, R.S. 2014. Time course of oocyte development in winter flounder (Pleuronectidae: *Pseudopleuronectes americanus*) and spawning seasonality for the Gulf of Maine, Georges Bank, and Southern New England stocks. J. Fish Biol. doi:10.1111/jfb.12431.

R Development Core Team. 2013. R: a language and environment for statistical computing [online]. R Foundation for Statistical Computing: Vienna, Austria. Available from http://www.R-project.org/.

Reid, R.N., Almeida, F.P., and Zetlin, C.A. 1999. Essential fish habitat source document: fishery-independent surveys, data sources, and methods. NOAA Technical Memorandum, NMFS-NE-122.

Ruß, G. 2012. Spatial data mining in precision agriculture. Ph.D. dissertation, Otto-von-Guericke-Universität Magdeburg.

Ruß, G., and Kruse, R. 2011. Exploratory hierarchical clustering for management zone delineation in precision agriculture. *In* Advances in data mining. Applications and theoretical aspects. *Edited by* P. Perner. Springer, Berlin. pp. 161–173.

Smart, T.I., Duffy-Anderson, J.T., Horne, J.K., Farley, E.V., Wilson, C.D., and Napp, J.M. 2012. Influence of environment on walleye pollock eggs, larvae, and juveniles in the southeastern Bering Sea. Deep-Sea Res. Part II Top. Stud. Oceanogr. **65–70**: 196–207. doi:10.1016/j.dsr2.2012.02.018.

Tobin, D., and Wright, P.J. 2011. Temperature effects on female maturation in a temperate marine fish. J. Exp. Mar. Biol. Ecol. **403**: 9–13. doi:10.1016/j.jembe.2011.03.018.

Wahba, G. 1981. Spline interpolation and smoothing on the sphere. SIAM J. Sci. Stat. Comput. **2**(1): 5–16. doi:10.1137/0902002.

Wirgin, I., Maceda, L., Grunwald, C., Roy, N.K., and Waldman, J.R. 2014. Coastwide stock structure of winter flounder using nuclear DNA analyses. Trans. Am. Fish. Soc. **143**: 240–251. doi:10.1080/00028487.2013.847861.

Wood, S.N. 2003. Thin plate regression splines. J.R. Statist. Soc. B Stat. Methodol. **65**(1): 95–114. doi:10.1111/1467-9868.00374.

Wood, S.N. 2006. Generalized additive models: an introduction with R. Chapman and Hall/CRC, Boca Raton, Fla.

Wood, S.N. 2011. Fast stable restricted maximum likelihood and marginal likelihood estimation of semiparametric generalized linear models. J.R. Statist. Soc. B Stat. Methodol. **73**(1): 3–36. doi:10.1111/j.1467-9868.2010.00749.x.

Wuenschel, M.J., Able, K.W., and Byrne, D. 2009. Seasonal patterns of winter flounder *Pseudopleuronectes americanus* abundance and reproductive condition on the New York Bight continental shelf. J. Fish Biol. **74**: 1508–1524. doi:10.1111/j.1095-8649.2009.02217.x. PMID:20735650.